An Aperture Back-Projection Technique and Measurements Made on a Flat Plate Array with a Spherical Near-Field Arch

Doren W. Hess [1], Scott McBride [2]

MI Technologies
1125 Satellite Boulevard, Suite 100
Suwanee, Georgia 30024, U.S.A.
[1]dhess@mi-technologies.com
[2]smcbride@mi-technologies.com

***Abstract*— We describe two theoretical bases for an algorithm for back-projection. The first is (1) Fourier inversion of the mathematical expression for the far electric field components in terms of the aperture electric field. The second is (2) Fourier inversion of the complete vectorial transmitting characteristic of Kerns' scattering matrix. It is this characteristic that results from the standard process of planar near-field (PNF) scanning and the ensuing reduction of the PNF transmission equation. We demonstrate that the theoretical approaches (1) and (2) yield identical back-projection algorithms. We report on back-projection measurements of an 18 inch X-band flat plate phased array using the far-field obtained from spherical near-field scanning. The spherical measurements were made on a large arch range.**

I. INTRODUCTION

This back-projection to an aperture with planar near-field scanning has been thoroughly explored. Its application to phased array element alignment and element diagnostics has found considerable success [1]. Back-projection of planar near-field scanning data, however, has drawbacks: Firstly, the unwanted presence of the standing wave between the array antenna and the near-field probe, and secondly, the limited aperture resolution due to scan-area truncation [2]. Recently, Cappellin et al have explored the utility of spherical scanning for reflector antenna back-projection and diagnostics [3]. Here we demonstrate with a flat-plate slotted array the utility of an arch scanner for obtaining reliable back-projection results.

We have employed two approaches for back-projection. The first is (1) Fourier inversion from the mathematical expression for the far electric field components in terms of the aperture electric field. The second is (2) Fourier inversion of the complete vectorial transmitting characteristic of Kerns' scattering matrix [**5**]. Here we describe and demonstrate an algorithm that estimates the near electric field from the far electric field in a manner equivalent to conventional PNF aperture imaging.

We report on back-projection measurements of an 18 inch X-band flat plate phased array using the far field obtained from spherical NF scanning. Because of the large 173 inch radius, the standing wave was significantly reduced; furthermore, data was acquired over all of the forward hemisphere, equivalent to a 90° critical angle, giving the greatest resolution in the aperture distribution available from the non-evanescent spectrum.

II. BACK-PROJECTION FROM FAR-FIELD APERTURE THEORY

The direct back-projection algorithm was implemented some time ago within the environment of the MI Technologies MI-3000 Data Acquisition and Analysis System to permit the aperture fields of a transmitting antenna to be reconstructed from far-field pattern data without employing any of the classic planar near-field routines. The basis of the algorithm can be found in the standard antenna textbook entitled "Antenna Theory: Analysis and Design" by C.A. Balanis [**4**]. There in Chapter 11 one finds the following relations that relate the far electric fields of an aperture to the equivalent current distributions within the aperture, which can be taken as directly proportional to the aperture fields themselves.

From equations 11-10 b,c, 11-12 c,d, 11-15c of Balanis and using $J_x, J_y, J_z, M_z, = 0$, we get

$$E_\theta \cong -\frac{jke^{-jkr}}{4\pi r}(L_\phi) \qquad E_\phi \cong +\frac{jke^{-jkr}}{4\pi r}(L_\theta) \qquad \text{(1a,b)}$$

$$L_\theta = \iint_{Aperture}[M_x\cos\theta\cos\phi + M_x\cos\theta\sin\phi]e^{jkr'\cos\psi}ds' \qquad \text{1c)}$$

$$L_\phi = \iint_{Aperture}[-M_x\sin\phi + M_x\cos\phi]e^{jkr'\cos\psi}ds' \qquad \text{(1d)}$$

$$r'\cos\psi = x'\sin\theta\cos\phi + y'\sin\theta\sin\phi \qquad \text{(1e)}$$

These equations relate the transverse components of the far electric field to the equivalent x- and y- directed source currents in the aperture. Here θ and ϕ are the polar and azimuthal direction angles from the aperture to the far-field point, with z as the polar axis, and the wave number k is given by the ration $2\pi/\lambda$, where λ is the free-space wavelength. (Note that the derivation in this section employs the $\exp(+j\omega t)$ time convention, following Balanis.)

Balanis' discussion of the principle of equivalent sources and his example of how to obtain the equivalent magnetic current from the aperture electric field in Section 11.2 makes it clear that the magnetic currents used to represent the aperture fields can be taken as proportional to the electric field components in the aperture as follows:

$$E_x^{Aperture} \propto M_y \qquad E_y^{Aperture} \propto M_x \tag{2a,b}$$

Furthermore, one can recognize the form of the integral expressions as two-dimensional Fourier transforms.

Thus, consistent with Balanis, (pg 461), the far-field components due to an aperture field $\boldsymbol{E}^{Aperture}$ are proportional to the Fourier transform ($\Im$) of a y'-polarized aperture electric field

$$\begin{aligned} E_{\theta'} &\propto \sin\phi' \Im(E_{y'}^{Aperture}) \\ E_{\phi'} &\propto \cos\theta' \cos\phi' \Im(E_{y'}^{Aperture}) \end{aligned} \tag{3a,b}$$

Similarly, for an x'-polarized aperture electric field the corresponding far-field components would be

$$\begin{aligned} E_{\theta'} &\propto \cos\phi' \Im(E_{x'}^{Aperture}) \\ E_{\phi'} &\propto -\cos\theta' \sin\phi' \Im(E_{x'}^{Aperture}) \end{aligned} \tag{3c,d}$$

In general, there might be both x'- and y'- polarized electric fields in the aperture and the far electric field would be the linear superposition of the two; so that

$$\begin{aligned} E_{\theta'} &\propto \cos\phi' \Im(E_{x'}^{Aperture}) + \sin\phi' \Im(E_{y'}^{Aperture}) \ ; \\ E_{\phi'} &\propto \cos\theta' (-\sin\phi' \Im(E_{x'}^{Aperture}) + \cos\phi' \Im(E_{y'}^{Aperture})) \ . \end{aligned} \tag{4a,b}$$

This pair of equations can be inverted to write

$$\begin{aligned} \Im(E_{x'}^{Aperture}) &\propto E_{\theta'} \cos\phi' - \frac{E_{\phi'}}{\cos\theta'} \sin\phi' \\ \Im(E_{y'}^{Aperture}) &\propto E_{\theta'} \sin\phi' + \frac{E_{\phi'}}{\cos\theta'} \cos\phi' \end{aligned} \tag{5a,b}$$

This then gives us the result we seek of how to take the far electric field and directly compute the fields in the aperture of the antenna that produced it. The algorithm is first to adjust the amplitude of the phi-component by the $\cos\theta$ factor and then to rotate the theta- and phi- components by the angle ϕ', prior to performing a two-dimensional inverse Fourier transform on each of the resulting data sets:

$$\begin{aligned} E_{x'}^{Aperture} &\propto \Im^{-1}[E_{\theta'} \cos\phi' - \frac{E_{\phi'}}{\cos\theta'} \sin\phi'] \\ E_{y'}^{Aperture} &\propto \Im^{-1}[E_{\theta'} \sin\phi' + \frac{E_{\phi'}}{\cos\theta'} \cos\phi'] \end{aligned} \tag{6a,b}$$

One important detail has yet to be mentioned, however. The natural independent variables of the far electric field components are the direction angles θ and ϕ; whereas the Fourier transform must be performed with the sine-space variables k_x and k_y. Thus, before the inverse Fourier transforms can be taken the data sets must be interpolated at equally spaced intervals in sine space rather than the naturally occurring equally spaced intervals of angular space.

Several techniques are available for this interpolation from an angular grid to a rectangular grid in K-space. The results shown here made use of a simple bilinear complex interpolation. The need for interpolation to the K-space grid allows us without penalty to specify a grid that will transform directly to a superset of the desired aperture grid.

III. Computation of the Aperture Electric Field from the Plane-Wave Spectrum

In this section we show that there is another line of reasoning based upon Kerns' plane wave spectrum theory of antennas [**5**] that leads to the same algorithm for computing the aperture field from the far-field components. (Note that the derivation in this section employs the exp(-iωt) time convention, following Kerns.)

It is customary in performing the planar near-field to far-field transform to arrive at the determination of the far electric field from the following asymptotic relationship:

$$\boldsymbol{E}(\boldsymbol{r}) \approx -i\gamma \, \boldsymbol{t}_{10}(\boldsymbol{R}k/r) \, a_0 e^{ikr}/r \tag{7}$$

Kerns, equation (1.6-1), where $\gamma = k\cos\theta$, and $\boldsymbol{t}_{10}$ is the complete transmitting characteristic of the antenna-under-test. In planar scanning, the quantity $\boldsymbol{t}_{10}$ is determined by de-embedding it from the coupling product that results from a two-dimensional Fourier transform of the *x*-*y* scanning data. This has the effect of removing the influence of the probe from the result. The complete transmitting characteristic is related to the partial or transverse transmitting characteristic, $\boldsymbol{T}_{10}$, as Kerns reminds us by his equation 1.6-3. (Following the now common convention, to connote the transmitting characteristic of the antenna under test (AUT), we employ here the symbols $\boldsymbol{t}$ and $\boldsymbol{T}$ for the transmitting characteristic rather than Kerns' original $\boldsymbol{s}$ and $\boldsymbol{S}$.) Taking the case of the right-hand hemisphere, we set $q=1$; and, we recall from Kerns that

$$\boldsymbol{t}_{10}(\boldsymbol{K}) = [k/\gamma] T_{10}(1,\boldsymbol{K}) \hat{\boldsymbol{e}}_{/\!/}(\boldsymbol{k}) + T_{10}(2,\boldsymbol{K}) \hat{\boldsymbol{e}}_{\perp}(\boldsymbol{K}) \, . \tag{8}$$

This result is made easier to understand by referring to the definitions of the unit vectors that appear here, which can be found in Kerns' Figure 3 and the footnotes to Table 1 on pp. 58 and 59.

$$\hat{\boldsymbol{e}}_{/\!/} = \hat{\boldsymbol{e}}_{\theta} \qquad \hat{\boldsymbol{e}}_{\perp} = \hat{\boldsymbol{e}}_{\phi} \tag{9a,b}$$

We should also remember that the complete radiated spectrum is related to the transmitting characteristic and the incident excitation a_0 by the simple relation

$$\boldsymbol{t}_{10}(\boldsymbol{K}) \, a_0 = \boldsymbol{b}_1(\boldsymbol{K}) \tag{10}$$

which is Kerns' equation (1.6-2).

The problem of how to compute the aperture field of a transmitting antenna from a knowledge of its plane-wave spectrum is made simple by referring to one of Kerns' results that occurs early in his development -- his equations (1.2-14) and (1.2-15a) -- that relate transverse quantities:

$$\boldsymbol{E}_{1t}(\boldsymbol{r}) = \frac{1}{2\pi} \int \boldsymbol{B}_1(\boldsymbol{K}) \, e^{i\gamma z} e^{i\boldsymbol{K} \circ \boldsymbol{R}} d\boldsymbol{K} \ , \tag{11}$$

$$\boldsymbol{B}_1(\boldsymbol{K}) = \sum_m b_1(m,\boldsymbol{K}) \boldsymbol{\kappa}_m \ . \tag{12}$$

The unit vectors $\boldsymbol{\kappa}_1$ and $\boldsymbol{\kappa}_2$ are defined by Kerns in his Figures 2 and 3 and are the polar 2-D unit vectors in the transverse *x-y* plane. Explicitly, from Kerns' Table 1,

$$\hat{\kappa}_1 = \hat{e}_x \cos\phi + \hat{e}_y \sin\phi \qquad (13a)$$

$$\hat{\kappa}_2 = -\hat{e}_x \sin\phi + \hat{e}_y \cos\phi = \hat{e}_\perp \qquad (13b)$$

What we now want to do is to relate the kappa-components of the transverse spectrum $\boldsymbol{B}_1(\boldsymbol{K})$ to the theta- and phi-components of $\boldsymbol{t}_{10}(\boldsymbol{K})$ as given by equations 8 and 9 above.

First write equation 12 explicitly in the kappa components

$$\boldsymbol{B}_1(\boldsymbol{K}) = \hat{\boldsymbol{\kappa}}_1(\hat{\boldsymbol{\kappa}}_1 \circ \boldsymbol{b}_1(\boldsymbol{K})) + \hat{\boldsymbol{\kappa}}_2(\hat{\boldsymbol{\kappa}}_2 \circ \boldsymbol{b}_1(\boldsymbol{K})) \qquad (14)$$

Next we obtain expressions for the components of $\boldsymbol{b}_1(\boldsymbol{K})$. From equation 10,

$$\frac{\boldsymbol{b}_1(\boldsymbol{K})}{a_0} = t_{10\theta}(\boldsymbol{K})\hat{\boldsymbol{e}}_\theta + t_{10\phi}(\boldsymbol{K})\hat{\boldsymbol{e}}_\phi \quad . \qquad (15)$$

And from Kerns, Table 1,

$$\hat{\boldsymbol{e}}_\phi = \hat{\kappa}_2 \; ; \quad \hat{\boldsymbol{e}}_\theta = \hat{\kappa}_1 \cos\theta - \hat{\boldsymbol{e}}_z \sin\theta \qquad (16a,b)$$

Combining equations 14,15,16 yields then an expression for the transverse spectrum in terms of its kappa components but expressed in terms of the theta and phi components of the complete transmitting characteristic:

$$\frac{\boldsymbol{B}_1(\boldsymbol{K})}{a_0} = \hat{\boldsymbol{\kappa}}_1[t_{10\theta}(\boldsymbol{K})\cos\theta] + \hat{\boldsymbol{\kappa}}_2[t_{10\phi}(\boldsymbol{K})] \qquad (17)$$

Equations 11 and 17 can now be combined to give an expression for the aperture field in terms of the theta and phi components of the complete vectorial spectrum and expressed in terms of the polar -- i.e. kappa-- components on the x-y aperture plane.

$$\boldsymbol{E}_{1t}(\boldsymbol{r}) = \frac{a_0}{2\pi}$$

$$\int\{\hat{\boldsymbol{\kappa}}_1[t_{10\theta}(\boldsymbol{K})\cos\theta] + \hat{\boldsymbol{\kappa}}_2[t_{10\phi}(\boldsymbol{K})]\}\, e^{i\gamma z} e^{i\boldsymbol{K}\circ\boldsymbol{R}} d\boldsymbol{K} \qquad (18)$$

These kappa unit vectors can be re-expressed in terms of the x- and y- unit vectors of the x-y aperture plane as in equation 13. The term in braces then becomes

$$\{\hat{\boldsymbol{\kappa}}_1[t_{10\theta}(\boldsymbol{K})\cos\theta] + \hat{\boldsymbol{\kappa}}_2[t_{10\phi}(\boldsymbol{K})]\} =$$

$$\{[t_{10\theta}(\boldsymbol{K})\cos\theta][\hat{\boldsymbol{e}}_x\cos\phi + \hat{\boldsymbol{e}}_y\sin\phi] +$$

$$[t_{10\phi}(\boldsymbol{K})][-\hat{\boldsymbol{e}}_x\sin\phi + \hat{\boldsymbol{e}}_y\cos\phi]\} \quad = \qquad (19)$$

$$\{\hat{\boldsymbol{e}}_x[t_{10\theta}(\boldsymbol{K})\cos\theta\cos\phi - t_{10\phi}(\boldsymbol{K})\cos\theta\frac{\sin\phi}{\cos\theta}] +$$

$$\hat{\boldsymbol{e}}_y[t_{10\theta}(\boldsymbol{K})\cos\theta\sin\phi + t_{10\phi}(\boldsymbol{K})\cos\theta\frac{\cos\phi}{\cos\theta}]\}$$

In view of the well known relationship between the far electric field and the complete vectorial transmitting characteristic, including the $\cos\theta$ factor, found in equation 7, the expression 18 for the transverse aperture field can be rewritten as equation 20 below. Note that the integral has the form of a two-dimensional Fourier transform; note also that for back-projection, $z=0$ This indeed has the exact same form as the earlier result from aperture theory, Section 2; please see equation 6 above.

$$\boldsymbol{E}_{1t}(\boldsymbol{r}) \propto$$

$$\int \{\hat{\boldsymbol{e}}_x[E_\theta(\boldsymbol{K})\cos\phi - E_\phi(\boldsymbol{K})\frac{\sin\phi}{\cos\theta}] + \qquad (20)$$

$$\hat{\boldsymbol{e}}_y[E_\theta(\boldsymbol{K})\sin\phi + E_\phi(\boldsymbol{K})\frac{\cos\phi}{\cos\theta}]\}e^{i\gamma z}e^{i\boldsymbol{K}\circ\boldsymbol{R}}d\boldsymbol{K}$$

Thus we have shown that in fact computing the aperture field directly from aperture theory and computing it from the theory of the plane wave spectrum as used in planar NF scanning give identical algorithms.

IV. Measured Near-Field Results and Examples of Back-Projection

At MI Technologies we have measured a flat plate slotted array by means of both planar and spherical NF scanning. This 18-inch diameter array operates at frequencies near 9.375 GHz; it is linearly polarized and has first sidelobes that lie approximately 30 dB below the main beam peak. A photograph of this antenna is shown in Fig. 1 along with a graphic overlay of the element map. For the purpose of the demonstration two of the elements were blocked with metalized mylar tape, as shown.

This antenna has also been used in the commissioning of a large spherical NF arch range. During arch-range checkout data was acquired in both polar and equatorial AUT orientations [6]. The polar orientation was achieved by pointing the aperture normal vertically, or aimed at $\theta = 0°$ in the far field. The equatorial orientation was achieved by pointing the aperture normal horizontally or aimed at $\theta = 90°$ in the far field. Figure 2 exhibits the comparison between the aperture back-projections in a common coordinate system obtained in the two different orientations. To obtain the aperture field from spherical NF data, first the far field is computed and then the direct method of Section 2 is employed. The result shows remarkable agreement both in amplitude and in phase. Any possible discrepancy due perhaps to mechanical distortion between the two orientations was clearly quite small to achieve the agreement illustrated.

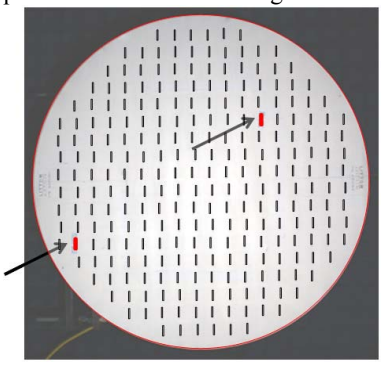

Fig. 1. Overlay of Element Map and Photograph of the 18 inch Flat Plate Array with the Blocked Elements Marked in Red

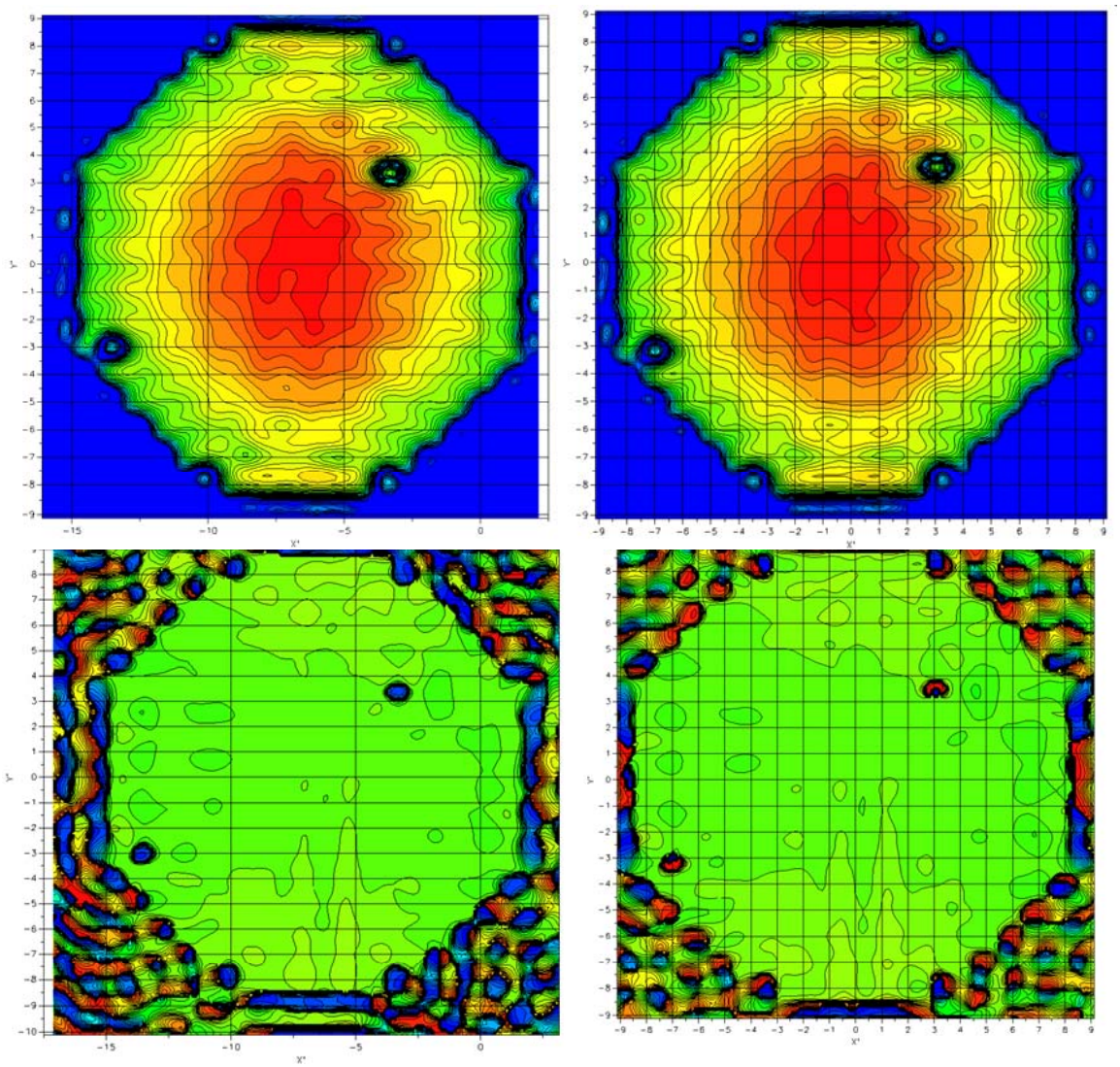

Fig. 3. Comparison Between Amplitude and Phase Distributions from Back-Projection of Spherical Near-Field Data for Polar and Equatorial Orientation of the Measurement Coordinate System

V. Conclusions

We have described a back-projection algorithm with far electric field as input and shown it to be consistent both with conventional antenna aperture theory and with Kerns' plane-wave scattering matrix theory. We have confirmed the agreement between the corresponding code sets using near-field measurements. We have also demonstrated the consistency and robustness of the method with spherical NF measurements made on a large arch range in polar and equatorial orientations.

References

[1] D. Garneski, "A new implementation of the planar near-field back projection technique for phased array testing and aperture imaging," in the 1990 Symposium Digest of The Antenna Measurement Techniques Association, pp. 9-9 - 9-14, Philadelphia, PA.

[2] A. C. Newell, B. Schluper, R.J. Davis, "Holographic projection to an arbitrary plane from spherical near-field measurements," in the 2001 Symposium Digest of the Antenna Measurement Technigues Association, pp. 92 - 97, Denver, CO.

[3] C. Cappellin, A. Frandsen, O.Breinbjerg, "Application of the SWE-to-PWE antenna diagnostics technique to an offset reflector antenna, *IEEE Antenna & Propagation Magazine*, Vol 50, pp.204-213, October 2008.

[4] C.A. Balanis, , *Antenna Theory: Analysis and Design,* 2nd Ed., Chapter 11, New York, NY, U.S.A. John Wiley and Sons,Inc., 1982.

[5] D.M. Kerns, "Plane-wave scattering matrix theory of antennas and antenna-antenna interactions," Boulder, CO, U.S. Dept of Commerce, National Bureau of Standards, NBS Monograph 162, June 1981.

[6] D.W. Hess, J.A. Fordham, S. Pierce, E. Langman, "Application of a circular arch for spherical near-field antenna measurements from 1 to 60 GHz, *28th ESA Antenna Measurement Workshop on Space Antenna Systems and Technologies*, Conference Proceedings, pp. 920-927, ESTEC, Noordwijk, The Netherlands, 31 May - 03 June 2005.